Int. J. Multiphase Flow, Vol. 1, pp. 647–669. Pergamon Press, 1974. Printed in Great Britain.

THE ANALYSIS OF A MECHANISM OF LIQUID REPLENISHMENT AND DRAINING IN HORIZONTAL TWO-PHASE FLOW

M. W. E. CONEY
Central Electricity Research Laboratories, Leatherhead, Surrey, England

(*Received* 20 *November* 1973)

Abstract—There is a regime of two-phase flow in which large waves or surges pass rapidly along a horizontal tube accompanied by splashing, wave-breaking and entrainment with the result that water is thrown to the upper surface of the tube. Between surges the film on the top surface is depleted by draining under gravity and by evaporation if the tube is heated. If the interval between surges is sufficiently long a dry patch may begin to form. In this paper, a theory is given for the calculation of the film thickness left behind on the top surface and for the calculation of the time to dryout. The theory includes both the effect of the boundary layer development during replenishment of the film and also the effect of the axial deceleration of the film at the point where the liquid replenishment ceases. Finally, the predicted variation of film thickness is compared with experimental film thickness traces obtained in this type of horizontal two-phase flow. The agreement is found to be very satisfactory. This analysis is of interest in connection with the prevention of permanent and intermittent dryout at low qualities in nuclear power station evaporators.

1. INTRODUCTION

One of the regimes of horizontal gas–liquid flow is characterized by the passage of large disturbances which maintain a liquid film on the upper surface of the tube. Such a disturbance appears to consist of a large breaking wave of foaming liquid, a portion of which is continually being splashed and sprayed onto the surface of the tube above the wave or thrown forward such that it falls into the liquid layer ahead of the oncoming wave. The liquid thrown to the upper surface forms a thick film which is so disturbed by surface waves and by impinging droplets that the whole tube usually becomes opaque for a distance of from 0.1 to 1.0 m. When the wave has passed, the film on the upper surface drains down the side walls of the tube and, unless another large disturbance arrives, the film eventually breaks down. In a heated tube, evaporation of the film causes a dry patch to form much sooner.

The above description is largely derived from an experimental study undertaken at the Central Electricity Research Laboratories using an atmospheric air–water facility with a horizontal test-section consisting of a perspex tube 51 mm in diameter. Visual observation and high speed cine film indicated the basic structure of the flow. Traces showing the variation with time of the film thickness on the upper surface of the tube were also obtained using the probe described by Coney (1973). In some tests a special technique was used to superimpose the film thickness traces onto the cine film so that the thickness variations could be related directly to the wetting events occurring simultaneously in the tube.

Other investigators have described similar phenomena in various two-phase systems, usually applying the term "slug flow" as a classification (e.g. Alves 1954; Baker 1954). Some excellent photographs are shown by Schicht (1969), who also describes the change in appearance of the flow with increasing gas velocity. A useful description of this type of flow is also given by Zahn (1964) who made a visual study of evaporating refrigerant R-22 in a horizontal tube approximately 12 mm in diameter. The term "slug flow" is avoided in this paper for two reasons: firstly, the term is often applied to another regime in which the gas flows in the form of large bullet-shaped bubbles. This type of flow can occur in a tube of any inclination. Secondly, the term "slug flow" may be taken to imply that the tube is blocked by liquid. In fact, it was found in the C.E.R.L. air–water facility that in the flow ranges of $8\text{ m/sec} \lesssim V_G \lesssim 20\text{ m/sec}$ and $0.3\text{ m/sec} \lesssim V_L \lesssim 1.5\text{ m/sec}$ the film thickness measured on the top surface rarely exceeded the maximum range of the probe which was 2.5 mm. (V_G and V_L are the gas and liquid superficial velocities, respectively.) This was also true at lower gas velocities (~ 5 m/sec), provided the liquid velocity was not too high (~ 0.4 m/sec). Further evidence that the tube is not blocked is given by the fact that when $V_G \gtrsim 8$ m/sec, the disturbance moves slower than the superficial velocity of the gas, and liquid entrainment is blown forward ahead of the disturbance. For these reasons, the disturbances described here are referred to as "surges".

Figure 1a shows a diagrammatic representation of the mechanisms by which surges are believed to distribute water to the upper surface of the tube. Figure 1b shows an idealized picture which is used as the model for the calculation presented in this paper. It is assumed that replenishment to the upper surface takes place uniformly over a finite length of tube. At the end of the surge the replenishment is assumed to cease abruptly. In the present analysis it is assumed that the forward velocity of the liquid replenishment striking the film on the top surface is the same as that of the surge. In practice, the liquid droplets may be slightly accelerated by the gas flow. On the other hand, if some of the replenishment arrives as a result of splashing against the side walls of the tube, the velocity could be lower than that of the surge. However, neither effect is thought likely to change the velocity by an amount comparable with the velocity of the surge. The further assumption that the momentum transfer due to the impinging droplets is much larger than that due to the shear forces of the gas flow, leads to the result that the velocity of the liquid outside the boundary layer in the film is the same as that of the surge.

As shown in figure 1b, the boundary layer of decelerated liquid begins its growth at the front of the surge. When replenishment ceases, only the boundary layer is left behind. The variation of thickness of the film after this point is determined by the change in the velocity profile, by viscous draining and by evaporation of liquid from the film. The analysis presented here, which takes account of all the processes described above, finally results in a prediction of the variation of the film thickness behind a surge. These predictions are then compared with draining curves which have been obtained experimentally in an unheated two-phase flow. Calculations, which include the effect of an applied heat flux are also performed, and these show how the time to dryout behind a surge varies as a function of the heat flux, tube radius and the physical properties of the gas and liquid phases.

The work described here is of interest in connection with the observation of permanent

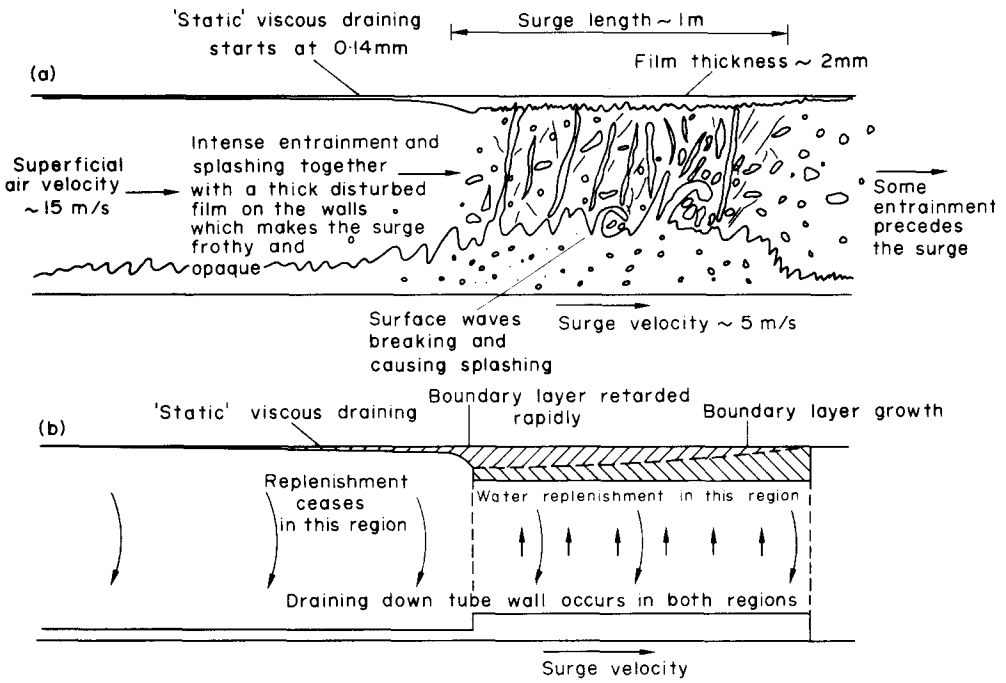

Figure 1. Pictorial representation of replenishment and draining processes (not to scale). (a) The situation as it is in practice with some typical dimensions and velocities. (b) The idealized picture.

and intermittent dryout at low heat fluxes in horizontal evaporator tubes containing a low quality ($\lesssim 25$ per cent) flow of steam and water. The observations were made by Lis & Strickland (1970) who used a high pressure facility to investigate the conditions which led to on-load corrosion in the horizontal evaporator tubes of one of the nuclear power stations of the CEGB (see Lunn & Harvey 1970). Flow regime studies at C.E.R.L. and elsewhere (e.g. Schicht 1969) and the evidence of experiments with vapour–liquid systems with density ratios near to that of steam and water at boiler pressures (Zahn 1964; Wedekind 1971), strongly support the idea that surges of the type described here are of importance in dryout phenomena.

2. DRAINING OF THE LIQUID FILM

Draining of the liquid film from the upper surface of the tube takes place both during the passage of the surge when replenishment occurs and also after the surge has passed and replenishment has ceased. Not only does it largely determine the rate of loss of liquid from the film, but it also has a profound effect on the development of the boundary layer. The problem of draining of a stationary film from the inside of a horizontal tube has been considered previously by Gardner (1972). The analysis of static draining given in this section is similar but has been modified in order to reduce the complexity of the boundary layer and film thickness calculations which follow.

Ignoring the curvature of the tube wall, except insofar as it affects the inclination Φ of the surface to the horizontal, drainage of a thin liquid film down the walls of a horizontal tube may be calculated by means of a simple balance between gravitational and viscous forces:

$$\Delta\rho\, g \sin\Phi(H - Y) = \rho\nu \frac{\partial W}{\partial Y}, \qquad [1]$$

where Y is the radial distance (m) measured inwards from the wall of the tube, H is the film thickness (m) and W (m/sec) is the velocity in the circumferential direction (see figure 2a); g is the gravitational acceleration (m/sec^2), ρ is the liquid density (kg/m^3); $\Delta\rho$ is the density difference between the two phases (kg/m^3) and ν is the kinematic viscosity of the liquid (m^2/sec). Integrating [1] we obtain

$$W = \frac{\Delta\rho g}{\rho\nu} \sin\Phi Y\left(H - \frac{Y}{2}\right). \qquad [2]$$

Differentiating with respect to Φ and taking the limit as $\Phi \to 0$:

$$\frac{\partial W}{\partial Z} = \frac{1}{R}\frac{\partial W}{\partial \Phi} = \frac{\Delta\rho g}{\rho R\nu} Y\left(H - \frac{Y}{2}\right), \qquad [3]$$

where Z is the distance in the direction tangential to the tube at $\Phi = 0$ and R is the tube radius (m).

These equations only apply when inertia effects are negligible. In practice, the velocity within the liquid film is limited by the maximum velocity W_m (m/sec) that the liquid could attain by free fall under gravity from the top of the tube. This velocity is given by

$$W_m = [2gR(1 - \cos\Phi)\Delta\rho/\rho]^{1/2}. \qquad [4]$$

Thus, the film thickness H_m (m) at which the surface velocity given by [2] reaches W_m is given by

$$H_m = \left[\frac{4\nu^2\rho R}{g\Delta\rho}\right]^{1/4} \quad \text{as } \Phi \to 0. \qquad [5]$$

Defining a parameter H_p:

$$\begin{aligned} H_p &= H \quad \text{if} \quad H \leqslant H_m \\ H_p &= H_m \quad \text{if} \quad H \geqslant H_m, \end{aligned} \qquad [6]$$

an approximate description of the draining behaviour of both thick and thin films may be obtained by assuming that

$$\frac{\partial W}{\partial Z} = \frac{\Delta\rho g}{\rho R\nu} Y\left(H_p - \frac{Y}{2}\right) \quad \text{for} \quad Y \leqslant H_m \qquad [7]$$

and

$$\frac{\partial W}{\partial Z} = \frac{\Delta\rho g}{\rho R\nu}\frac{H_m^2}{2} \quad \text{for} \quad Y \geqslant H_m. \qquad [8]$$

Equation [8] has been obtained by differentiating [4] with respect to Φ, substituting [5] and taking the limit as $\Phi \to 0$.

3. THE BEHAVIOUR OF THE BOUNDARY LAYER

In figure 1b, a boundary layer is seen to form in the film above the surge, where replenishment is taking place. In the following analysis it is assumed that the boundary layer is laminar. This assumption is examined in Appendix 1 where it is shown that transition to a turbulent boundary layer is unlikely except when the surge velocity is very high (~ 8 m/sec in an air–water system). In this section it is shown that the growth of the boundary layer is limited by the effects of draining so that (provided the region of replenishment is long enough) a stable velocity profile is obtained. However, if the liquid film is significantly thinner than the maximum thickness that the boundary layer can attain, the velocity profile of the stable boundary layer is severely modified. When replenishment ceases, the boundary layer, whatever its profile, becomes the film. However, the same type of boundary layer analysis can be applied in this region also.

Viscous draining plays an important part in both regions. Evaporation on the other hand, which is assumed to take place from the surface of the film rather than as a result of nucleate boiling, is only given special consideration where replenishment has ceased. Where there is replenishment, the effect of evaporation could be considered by simply subtracting the appropriate quantity to give a net rate of liquid replenishment to the upper surface. In practice, however, it is easier to measure an approximate average thickness of the film above a surge than it is to estimate the rate of replenishment. A film of known, constant thickness is therefore chosen as the starting point of the analysis.

3.1 *The modified boundary layer equations*

It is convenient for the purposes of the analysis to consider the surge to be stationary and the tube wall to be moving with a velocity U_o (m/sec). Thus, the idealized profiles of the surge and the associated liquid film do not change with time. This situation is illustrated in figure 2b. The growth of the boundary layer of thickness B on the upper surface of the horizontal tube is essentially a three dimensional problem. The boundary layer equations are (Schlichting 1968, p. 239)

$$\frac{\partial U}{\partial X} + \frac{\partial V}{\partial Y} + \frac{\partial W}{\partial Z} = 0 \qquad [9]$$

and

$$U\frac{\partial U}{\partial X} + V\frac{\partial U}{\partial Y} + W\frac{\partial U}{\partial Z} = -\frac{1}{\rho}\frac{\partial P}{\partial X} + \nu\frac{\partial^2 U}{\partial Y^2} \qquad [10]$$

where X is the distance measured in the axial direction, U, V and W are the velocities in the X, Y and Z directions and P is the pressure (N/m^2). Since we are only concerned with the position $\Phi = 0$, by symmetry W must vanish. Also, the pressure gradient is assumed to be negligible (Appendix I).

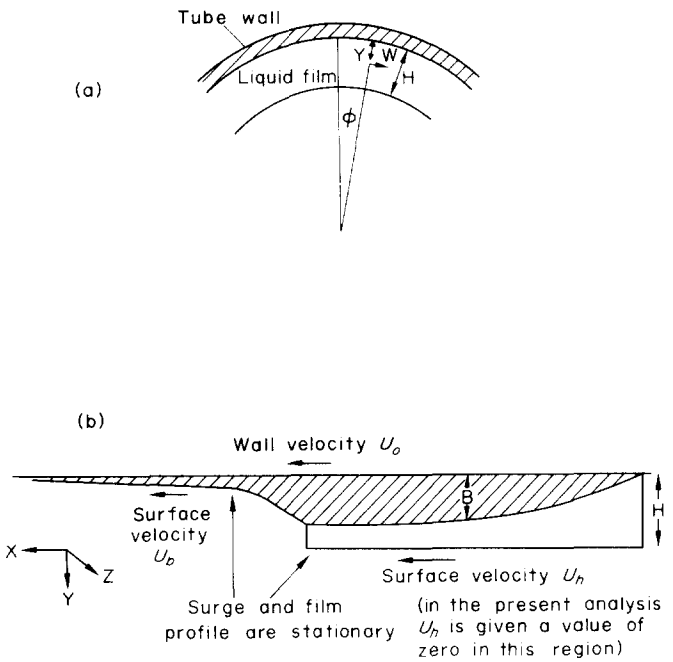

Figure 2. Illustration of certain parameters in the problem.

Introducing the non-dimensional distances

$$x = X/H_m, \quad y = Y/H_m, \quad z = Z/H_m \tag{11}$$

and

$$h = H/H_m, \quad h_p = H_p/H_m, \tag{12}$$

also the non-dimensional velocities

$$u = UH_m/\nu, \quad v = VH_m/\nu, \quad w = WH_m/\nu, \tag{13}$$

[9] and [10] reduce to

$$\frac{\partial u}{\partial x} + \frac{\partial v}{\partial y} + \frac{\partial w}{\partial z} = 0, \tag{14}$$

$$u\frac{\partial u}{\partial x} + v\frac{\partial u}{\partial y} = \frac{\partial^2 u}{\partial y^2} \tag{15}$$

and [7] and [8] become:

$$\frac{\partial w}{\partial z} = 2y(2h_p - y) \quad \text{when} \quad y \leqslant 1, \tag{16}$$

$$\frac{\partial w}{\partial z} = 2 \quad \text{when} \quad y \geqslant 1, \tag{17}$$

where h_p has the property that $h_p = h$ if $h \leqslant 1$ and $h_p = 1$ if $h \geqslant 1$.

3.2 *The momentum integral approximation*

An approximate solution to the boundary layer equations, [14] and [15], may be obtained by applying a modified version of the momentum integral method of Pohlhausen and von Karman (Schlichting 1968, p. 145). Integrating [14], using [16] and [17] we obtain for the cases where $y \leqslant 1$, $y \geqslant 1$ respectively

$$v = -\int_o^y \frac{\partial u}{\partial x}\,dy - 2y^2 h_p + \frac{2}{3}y^3, \qquad [18]$$

and

$$v = -\int_o^y \frac{\partial u}{\partial x}\,dy + \frac{2}{3} - 2y. \qquad [19]$$

Having obtained expressions for v, the momentum equation [15] is integrated over the dimensionless boundary layer thickness b. Thus

$$\int_o^b \left(u\frac{\partial u}{\partial x} + v\frac{\partial u}{\partial y}\right) dy = -\left(\frac{\partial u}{\partial y}\right)_{y=0}, \qquad [20]$$

since $\dfrac{\partial u}{\partial y} = 0$ at $y = b$.

Before substituting v into [20] we note that by integrating by parts

$$\int_o^b \frac{\partial u}{\partial y}\left(\int_o^y \frac{\partial u}{\partial x}dy\right) dy = u_b \int_o^b \frac{\partial u}{\partial x}dy - \int_o^b u\frac{\partial u}{\partial x}dy \qquad [21]$$

where $u = u_b$ at $y = b$.

From [18]–[21] we find that the expression

$$2\int_o^b u\frac{\partial u}{\partial x}dy - u_b\int_o^b \frac{\partial u}{\partial x}dy + \left(\frac{\partial u}{\partial y}\right)_{y=0}$$

is equal to

$$\int_o^b \left(2y^2 h_p - \frac{2}{3}y^3\right)\frac{\partial u}{\partial y}dy \quad \text{for} \quad b \leqslant 1 \qquad [22]$$

or equal to

$$\int_o^1 \left(2y^2 - \frac{2}{3}y^3\right)\frac{\partial u}{\partial y}dy + \int_1^b \left(2y - \frac{2}{3}\right)\frac{\partial u}{\partial y}dy \quad \text{if} \quad b \geqslant 1. \qquad [23]$$

3.3 *The velocity profile in the boundary layer*

At this stage it is necessary to assume a velocity profile for the boundary layer. We assume a profile of the form (Schlichting 1968, p. 192):

$$u = u_o + a_1 y + a_2 y^2 + a_3 y^3 + a_4 y^4, \qquad [24]$$

where u_o is the dimensionless velocity at $y = 0$, and a_1 to a_4 are constants which are determined by the boundary conditions. These are that, at the wall where $y = 0$, u equals

u_o and that since $\partial u/\partial x = 0$ and $v = 0$, then from [15], $\partial^2 u/\partial y^2$ is also zero at $y = 0$. Also at the edge of the boundary layer where $y = b$, $u = u_b$, and if the shear at this point is zero, then $\partial u/\partial y = 0$. Also, if u_b is a constant then from [15] $\partial^2 u/\partial y^2 = 0$ at $y = b$. It may be shown that with these conditions, [24] becomes

$$u = u_o - (u_o - u_b)\left(2\frac{y}{b} - 2\frac{y^3}{b^3} + \frac{y^4}{b^4}\right). \qquad [25]$$

This profile is assumed in all the following calculations, except for the stable boundary layer, in which case the velocity profile is calculated.

In some of these calculations u_b is allowed to vary, which means that the condition $\partial^2 u/\partial y^2 = 0$ no longer applies at $y = b$. In this case the profile should strictly be modified from [25], but since this would involve a considerable complication of the theory to avoid errors which are probably not very significant, it is assumed that [25] is valid throughout. It may be shown that substitution of [25] into [22] and [23] yields:

$$\frac{b^2}{2}\frac{\mathrm{d}u_b}{\mathrm{d}x}\frac{\left[\frac{74}{315}u_o + \frac{293}{630}u_b\right]}{(u_o - u_b)} + \frac{b}{2}\frac{\mathrm{d}b}{\mathrm{d}x}\left[\frac{23}{126}u_o + \frac{74}{630}u_b\right] + f_1(b) - 1 = 0 \qquad [26]$$

where
$$f_1(b) = b^3\left(\frac{2h_p}{15} - \frac{b}{42}\right) \quad \text{if} \quad b \leqslant 1, \qquad [27]$$

but
$$f_1(b) = \frac{3b^2}{10} - \frac{b}{3} + \frac{1}{6} - \frac{1}{30b^2} + \frac{1}{105b^3} \quad \text{if} \quad b \geqslant 1. \qquad [28]$$

4. THE BOUNDARY LAYER ABOVE THE SURGE

In this region, provided the growth of the boundary layer has not been limited by the thickness of the film, the velocity at the edge of the boundary layer is constant, so that

$$\mathrm{d}u_b/\mathrm{d}x = 0.$$

Hence, from [26]

$$\int_o^b \frac{b\,\mathrm{d}b}{1 - f_1(b)} = \frac{2x}{\left(\frac{23}{126}u_o + \frac{74}{630}u_b\right)}. \qquad [29]$$

If the effect of draining on the boundary layer growth can be ignored, $f_1(b)$ becomes negligible, so from [29]

$$b = \left[\frac{4x}{\left(\frac{23}{126}u_o + \frac{74}{630}u_b\right)}\right]^{1/2}. \qquad [30]$$

Two special cases are worth noting. Firstly, if $u_b = 0$ (which is the case of most importance in the present analysis), then

$$b = 4.681\sqrt{\frac{x}{u_o}}. \qquad [31]$$

This result has been obtained previously by Sakiadis (1961). Secondly, if $u_o = 0$, it is found that the boundary layer grows more rapidly and

$$b = 5.836\sqrt{\frac{x}{u_b}}. \qquad [32]$$

Equation [32] is the momentum integral approximation to the problem of the laminar boundary layer on a flat plate. The velocity profile obtained from [25] using [32] may therefore be compared with the exact solution, which is given by Schlichting (1968, p. 129). It is seen from table 1 that the agreement between the two solutions is excellent.

To obtain the boundary layer thickness as a function of distance in the case where draining takes place, [29] has been integrated numerically to give b as a function of the parameter ε, where

$$\varepsilon = \frac{2x}{\left(\frac{23}{126}u_o + \frac{74}{630}u_b\right)}. \qquad [33]$$

The results are shown in figure 3, which also includes for comparison, the function [30] which would have been obtained in the absence of draining. It is seen that draining has the important effect of progressively retarding further growth as the boundary layer thickness

Table 1. Comparison between the momentum integral approximation and the exact solution for a boundary layer on a flat plate

$y\sqrt{\frac{x}{u_b}}$	$\frac{u}{u_b}$ (exact)	$\frac{u}{u_b}$ (approx)
0.2	0.0664	0.0685
0.4	0.1328	0.1365
0.8	0.2647	0.2694
1.0	0.3298	0.3335
1.4	0.4563	0.4555
2.0	0.6298	0.6187
2.4	0.7290	0.7120
3.0	0.8461	0.8262
4.0	0.9555	0.9474
5.0	0.9916	0.9942
5.8	0.9984	0.9995

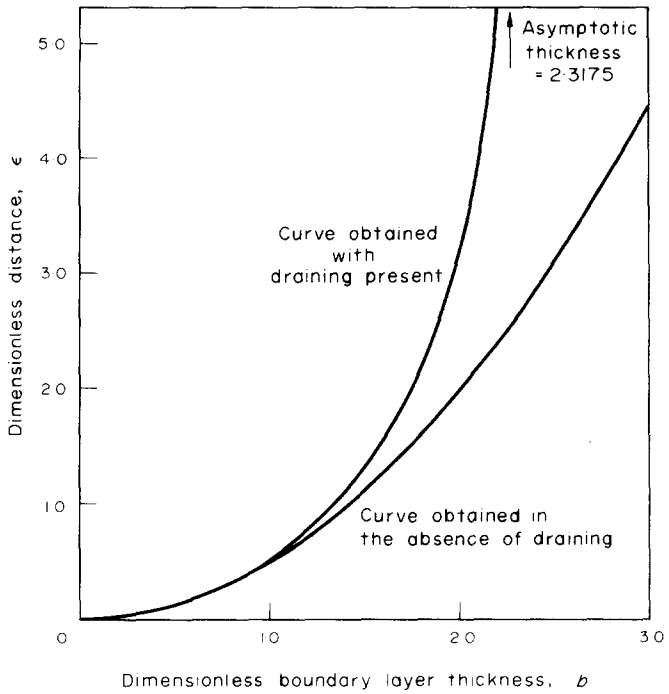

Figure 3. Comparison of boundary layer growth with and without the effect of draining.

increases. It can be seen from [28] and [29] that the boundary layer reaches an asymptotic thickness given by

$$\frac{3b^2}{10} - \frac{b}{3} - \frac{5}{6} - \frac{1}{30b^2} + \frac{1}{105b^3} = 0 \qquad [34]$$

which has a solution $b_{\max} = 2.3175$. It should be noted that this behaviour is closely analogous to that of boundary layer suction, which also results in an asymptotic thickness.

Typical parameters for an atmospheric air–water flow are $\Delta\rho = 10^3\ \mathrm{kg/m^3}$, $\nu = 8 \times 10^{-7}\ \mathrm{m^2/sec}$, $R = 0.025$ m. Hence, from [5], $H_m = 0.284$ mm. With $u_b = 0$, the parameter ε is given by

$$\varepsilon = 11.0\frac{x}{u_o} = 11.0\frac{\nu}{H_m^2}\frac{X}{U_o} = 109\ T_s \qquad [35]$$

where T_s is the time (sec) for the surge to pass a given point. Film thickness traces show that T_s is typically between 0.1 and 0.3 sec. Thus ε generally lies between 10 and 30, which suggests (see figure 3) that the boundary layer at the end of a surge in air–water flow is always close to its asymptotic thickness of 0.66 mm, provided the replenishment rate to the upper surface is sufficient to maintain a film thickness greater than this value.

5. THE BOUNDARY LAYER GROWTH LIMITED BY FILM THICKNESS

5.1 *Change in the velocity profile of the boundary layer*

The analysis of the previous section involved the assumption that at $y = b$

$$\partial u/\partial y = 0, \quad \partial^2 u/\partial y^2 = 0. \tag{36}$$

However, this is only true if the film thickness is greater than the boundary layer thickness, so that there is a body of liquid with a velocity u_b outside the boundary layer. However, if the replenishment rate is low enough, such that $h < b_{max}$, then a point is reached where the conditions [36] no longer apply. Under these circumstances it is seen from [15] that at $y = h$,

$$v(\partial u/\partial y) = \partial^2 u/\partial y^2 = \lambda, \tag{37}$$

where λ is a parameter which may be introduced to develop another polynomial approximation to the boundary layer profile. The special case $\lambda = 0$ corresponds to the profile given by [25]. Once the boundary layer thickness equals the film thickness, further development can only take place by modification of the profile according to [37], with the value of λ increasing from zero and approaching some asymptotic value.

The analysis of the change in the boundary layer profile is not pursued here because it is unlikely that this part of the process is of practical interest. This is because the boundary layer develops rapidly and it has already been seen that in most cases it is likely that it achieves a stable profile before the end of the surge. In the following section it is shown how this stable velocity profile may be calculated directly.

5.2 *The stable asymptotic boundary layer*

The transverse velocity in the stable boundary layer (expressed in dimensionless form) may be obtained from [18] and [19]:

$$v = -2y^2\left(h_p - \frac{y}{3}\right) \quad \text{for} \quad y \leqslant 1, \tag{38}$$

$$v = -2\left(y - \frac{1}{3}\right) \quad \text{for} \quad y \geqslant 1. \tag{39}$$

Also, from [15] $$v(\mathrm{d}u/\mathrm{d}y) = \mathrm{d}^2u/\mathrm{d}y^2. \tag{40}$$

if $h \leqslant 1$, then $h_p = h$ and integrating [40] using [38] it is found that

$$(u_o - u)/(u_o - u_h) = I_1(y)/I_1(h), \tag{41}$$

where u_h is the value of u at $y = h$ and where

$$I_1(\psi) = \int_o^{\psi} \exp -\frac{2}{3}y^3\left(h_p - \frac{y}{4}\right)\mathrm{d}y. \tag{42}$$

ψ is an arbitrary constant with the limits $0 \leqslant \psi \leqslant 1$.

If $h \geqslant 1$, then $h_p = 1$ and for $y \leqslant 1$, it is found that

$$(u_o - u)/(u_o - u_1) = I_1(y)/I_1(1), \tag{43}$$

where u_1 is the value of u at $y = 1$. Also for $y \geqslant 1$, it is found from [39] and [4] that

$$(u_1 - u)/(u_1 - u_h) = I_2(y)/I_2(h) \tag{44}$$

where

$$I_2(\psi) = \int_1^{\psi} \exp\left(-y^2 + \frac{2}{3}y + \frac{1}{3}\right) \mathrm{d}y, \tag{45}$$

and $\psi \geqslant 1$. A further necessary condition is that $\mathrm{d}u/\mathrm{d}y$ is continuous over the region where $y = 1$. Thus

$$(u_1 - u_h)/(u_o - u_1) = I_2(h)e^{-1/2}/I_1(1). \tag{46}$$

Eliminating u_1 it is found from [43] and [46] that for $y \leqslant 1$,

$$\frac{u_o - u}{u_o - u_h} = \frac{I_1(y)}{I_1(1) + I_2(h)e^{-1/2}}, \tag{47}$$

and from [44] and [46], for $y \geqslant 1$

$$\frac{u_o - u}{u_o - u_h} = \frac{I_1(1) + I_2(y)e^{-1/2}}{I_1(1) + I_2(h)e^{-1/2}}. \tag{48}$$

The displacement and momentum thicknesses δ_1, δ_2 of the stable boundary layer are defined as follows.

$$\delta_1 = \int_o^h \left(\frac{u - u_h}{u_o - u_h}\right) \mathrm{d}y, \tag{49}$$

$$\delta_2 = \int_o^h \left(\frac{u - u_h}{u_o - u_h}\right)^2 \mathrm{d}y. \tag{50}$$

These two quantities represent the respective thicknesses measured from a frame of reference travelling with a velocity u_h. The displacement thickness δ_1 is clearly related to the total flow f_L of liquid out of the surge into the film left behind.

$$f_L = \int_o^h u \, \mathrm{d}y = (u_o - u_h)\delta_1 + hu_h. \tag{51}$$

The case of greatest practical interest is that of $u_h = 0$, when in the absence of draining and evaporation, the film left behind by the surge tends to a thickness δ_1 because of the acceleration of the whole film up to a velocity u_o.

5.3 *Solution of the equations for a stable boundary layer*

Equations [41]–[50] have been solved for films of different thicknesses by means of a simple computer program. Figure 4 shows the stable displacement and momentum thicknesses as a function of the film thickness above the surge, which from here onwards

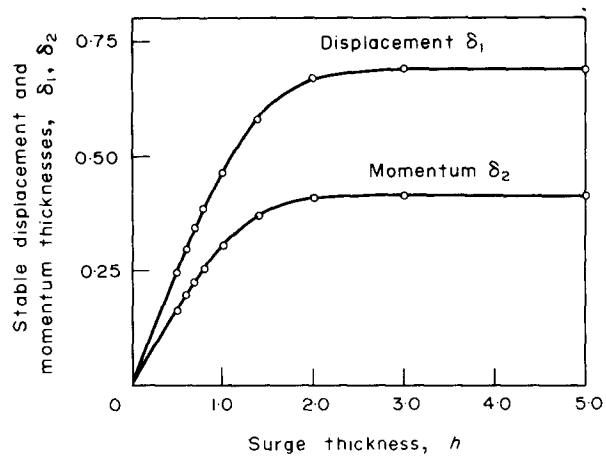

Figure 4. The stable displacement and momentum thicknesses as a function of the film thickness above the surge.

will be denoted h_s to avoid confusion with the thickness of the film left behind by the surge. As expected from the analysis on the growth of the boundary layer, the displacement thickness approaches an asymptotic value which it cannot exceed because of the draining of liquid from the boundary layer. The value obtained (0.689) is close to the expected value (0.695), which is the displacement thickness corresponding to the asymptotic thickness shown in figure 3.

Figure 5 shows the stable velocity profile as a function of y/h_s for films of various thicknesses. With thin films the velocity profile is almost linear, but with thick films the boundary layer occupies only a part of the film.

5.4 *Comparison of the stable velocity profile with the approximate profile*

When the liquid film thickness h_s above the surge is greater than about 2.0 it is expected that there is close agreement between the stable velocity profile and the approximation of [25], because the boundary conditions on the profile are approximately correct. However, at low values of h_s, the stable profile becomes progressively more linear, as shown in figure 5. When the boundary layer leaves the surge it is no longer subjected to the drag caused by liquid replenishment on the surface, and so in those cases where the stable profile differs from the approximate profile, the profile changes back to a form close to that given by [25].

In the calculation of the behaviour of the boundary layer behind a surge, it is assumed that the behaviour of the film may be represented by a profile of the same form as [25], but with the same initial film thickness b_i and displacement thickness δ_1 as that of the appropriate stable profile. If the displacement thickness of the stable profile δ_1 is greater that 0.3 h_s (which is the displacement thickness obtained from [25] and [49] when $h_s = b$),

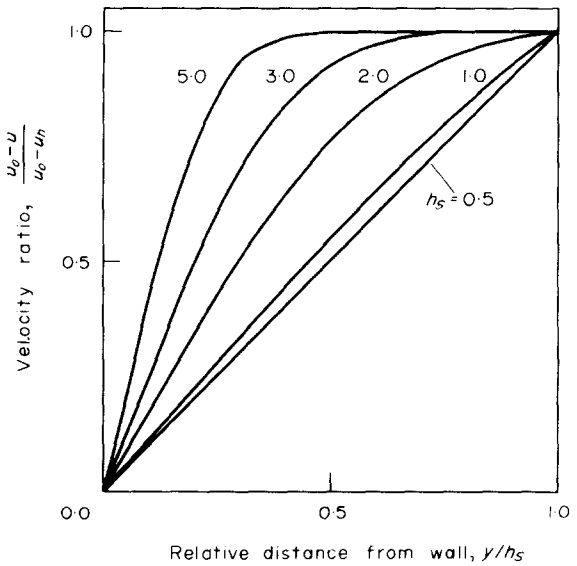

Figure 5. The stable velocity profile for different film thicknesses above the surge.

the correct displacement thickness is achieved by introducing an effective value of u_b, namely u_b^*, such that

$$\frac{u_o - u_b^*}{u_o - u_b} = \frac{10}{7}\left(1 - \frac{\delta_1}{b_i}\right). \qquad [52]$$

Thus, the initial profile [25] is modified to

$$u_r = \frac{10}{7}\left(1 - \frac{\delta_1}{h_s}\right)\left(\frac{2y}{h_s} - \frac{2y^3}{h_s^3} + \frac{y^4}{h_s^4}\right) \quad \text{if} \quad \delta_1 > 0.3\, h_s \qquad [53]$$

where

$$u_r = (u_o - u)/(u_o - u_b). \qquad [54]$$

In the cases where $\delta_1 < 0.3\, h_s$ it is assumed that the profile is initially given by [25] with $b_i = \delta_1/0.3$ and that in the region $b_i \leqslant y \leqslant h_s, u = u_b = 0$. Table 2 shows a comparison between the stable and the approximate profile for $h_s = 2.0$ and 3.0. It was found that both profiles for $h_s = 5.0$ differed from the corresponding profiles for $h_s = 3.0$ by less than 0.1 per cent, so these were not included. It is seen from table 2 that there is very close agreement between the stable and the approximate profile for $h_s = 3.0$. In the case of $h_s = 2.0$, where the velocity profile has been calculated from [53], the agreement is not so good, there being a maximum error of about 5 per cent.

Applying the ideas of this section, it is possible to calculate the initial values of the boundary layer thickness b_i and the effective velocity u_b^* at the edge of the boundary layer (for the case where the initial value of u_b is zero). These parameters are plotted in figure 6 versus the film thickness h_s above the surge.

Table 2

Distance from wall	Stable profile u_r for $h_s = 2.0$	Approx profile u_r for $h_s = 2.0$	Stable profile u_r for $h_s = 3.0$	Approx profile u_r for $h_s = 3.0$
0.2	0.1724	0.1884	0.1702	0.1729
0.4	0.3420	0.3667	0.3375	0.3387
0.6	0.5021	0.5269	0.4956	0.4915
0.8	0.6448	0.6633	0.6364	0.6268
1.0	0.7631	0.7726	0.7532	0.7416
1.2	0.8539	0.8535	0.8428	0.8342
1.4	0.9182	0.9072	0.9063	0.9042
1.6	0.9603	0.9372	0.9478	0.9526
1.8	0.9858	0.9491	0.9730	0.9819
2.0	1.0000	0.9509	0.9870	0.9960
2.2	—	—	0.9942	0.9985
2.6	—	—	0.9992	1.0000
3.0	—	—	1.0000	1.0000

6. THE BEHAVIOUR OF THE FILM LEFT BEHIND BY A SURGE

6.1 *Theory*

It is assumed that behind the surge liquid replenishment to the film has ceased so that, if the shear stresses of the gas phase may be neglected, the film must diminish in thickness as it is accelerated up to the velocity of the wall. This effect is, of course, in addition to the reduction of the film thickness due to draining and evaporation. The acceleration of the film is taken into account by allowing u_b to increase. Thus, with the assumption that the departure from the condition $\partial^2 u/\partial y^2 = 0$ at $y = b$ (caused by the variation of u_b) may

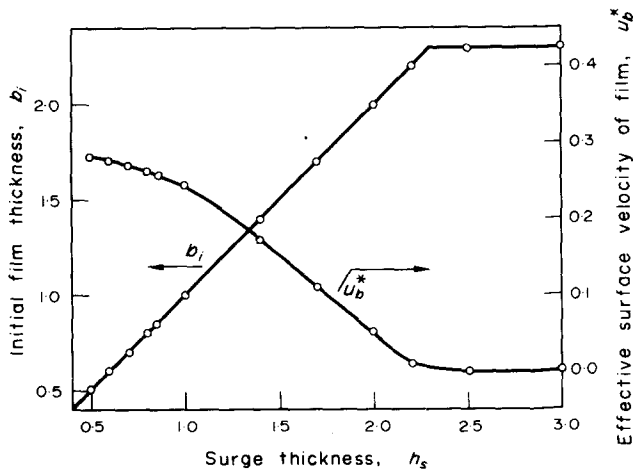

Figure 6. Variation of the initial film thickness and surface velocity with film thickness above the surge.

be ignored, the momentum equation is expressed by [26]–[28] with the added condition that, since the boundary layer is the film, $b = h$.

In addition, it is necessary to derive an equation expressing the conservation of the liquid

$$\frac{\mathrm{d}}{\mathrm{d}x}\left[\int_o^b u\,\mathrm{d}y\right] + \int_o^b \frac{\mathrm{d}w}{\mathrm{d}z}\,\mathrm{d}y + q = 0 \qquad [55]$$

where q is a dimensionless parameter expressing the rate of evaporation

$$q = \frac{QH_m}{\rho L v} \qquad [56]$$

and where Q is the heat flux (W/m^2) and L is the latent heat of evaporation (J/kg). From [55], [16], [17] and [25] it is seen that

$$\left(\frac{3}{10}u_o + \frac{7}{10}u_b\right)\frac{\mathrm{d}b}{\mathrm{d}x} + \frac{7}{10}b\frac{\mathrm{d}u_b}{\mathrm{d}x} + q + f_2(b) = 0 \qquad [57]$$

where $$f_2(b) = \tfrac{4}{3}b^3 \quad \text{if} \quad b \leqslant 1 \quad , \quad f_2(b) = 2b - \tfrac{2}{3} \quad \text{if} \quad b \geqslant 1. \qquad [58, 59]$$

The behaviour of the film outside the surge must be found by the simultaneous solution of the momentum equation [26] and the conservation equation [57]. In doing this, it is convenient to express the equations in terms of the film thickness ($h = b$) as measured by a probe fixed to the walls of the tube at a dimensionless time t, ($t = T/T_m$), where T is actual time (sec) and T_m is a characteristic time (sec) given by

$$T_m = H_m^2/v. \qquad [60]$$

Thus, $\mathrm{d}/\mathrm{d}t = u_o(\mathrm{d}/\mathrm{d}x)$ and [26] and [57] become

$$(f_1 - 1)\,\omega\frac{\mathrm{d}t}{\mathrm{d}b} - \frac{b^2}{2}\left(\frac{7}{10} - \frac{293}{630}\omega\right)\frac{\mathrm{d}\omega}{\mathrm{d}b} = \frac{b}{2}\omega\left(\frac{74\omega}{630} - \frac{3}{10}\right) \qquad [61]$$

$$(f_2 + q)\frac{\mathrm{d}t}{\mathrm{d}b} - \frac{7}{10}b\frac{\mathrm{d}\omega}{\mathrm{d}b} = \frac{7}{10}\omega - 1 \qquad [62]$$

where f_1 and f_2 are given by [27] and [58] or [28] and [59] as appropriate, and $\omega = 1 - u_b/u_o$.

Initial values of ω and b are chosen such that $\omega = 1 - u_b^*/u_o$ and $b = b_i$ when $t = 0$, where u_b^* and b_i are given as functions of h_s in figure 6. Equations [61] and [62] may now be solved to find the variation of b and ω with t. The dimensionless dryout time t_d is the time t when the film thickness b becomes zero.

6.2 *Solution of the equations*

Equations [61] and [62] were solved numerically to give draining curves, the shape of which is determined by the film thickness h_s above the surge and the heat flux parameter q. Figure 7 shows the effect of changing h_s when $q = 0$ and also the effect of two different values of q for the case of $h_s > 2.3$, which is referred to as the principal dynamic curve. Since it is found in practice that the vast majority of surges cause film thicknesses greater

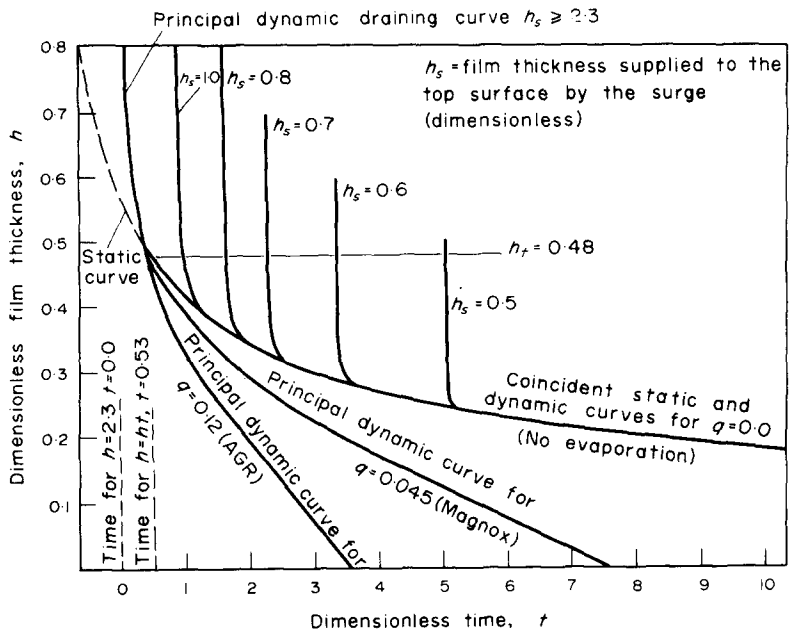

Figure 7. Various calculated draining curves which show the effect of the film thickness supplied by a surge, the effect of heat flux and the effect of making the assumption of a static film.

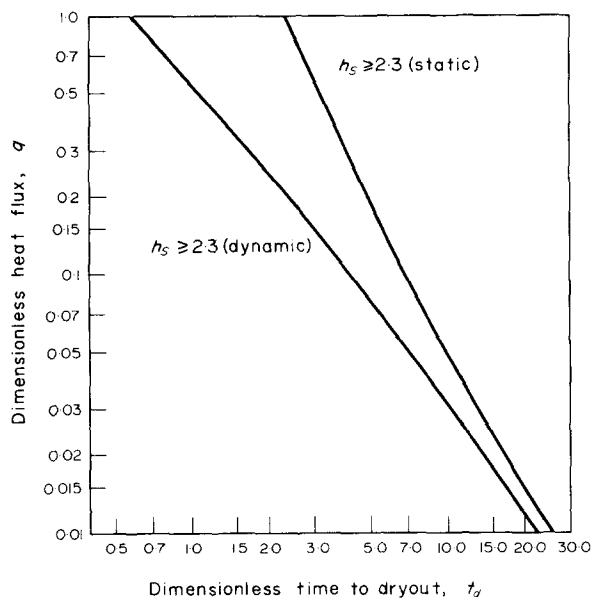

Figure 8. The calculated variation of the dimensionless dryout time t_d with dimensionless heat flux q.

than 2.3 H_m, this is the curve of greatest interest. The values of q chosen correspond to typical values for horizontal evaporators in Magnox and AGR power stations. Figure 7 also shows the "static" draining curve which is obtained if the effects of the boundary layer development and the axial velocity profile are ignored. The equations for static draining are described in Appendix 2. It is seen from figure 7 that the static and dynamic curves coincide at a thickness $h_t = 0.48$, if it is defined as the point at which the gradients of the two curves are within 10 per cent of each other.

Figure 8 shows the calculated variation of the time to dryout for the case of a thick film above the surge ($h_s \geqslant 2.3$). The dryout time is measured from the point where replenishment ceases. The comparison between the static and dynamic curves shows that the dynamic effects are particularly important at high heat fluxes.

6.3 *Comparison with experiment*

Figure 9 shows experimental film thickness traces obtained on the upper surface of a 51 mm diameter horizontal perspex tube containing an air–water flow at 30°C. Under

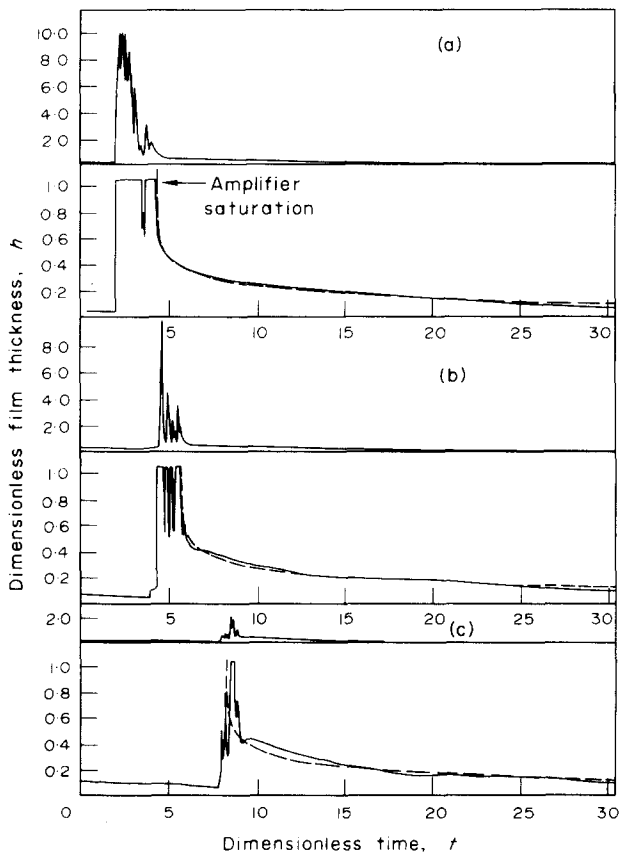

Figure 9. Comparison of the theoretical dynamic curve for $h_s > 2.3$ (which is shown by the dotted lines) with experimental traces.

these conditions $H_m = 0.285$ mm and $T_m = 0.102$ sec. Three examples are shown of wetting events observed when the gas and liquid superficial velocities were 4.0 and 0.3 m/sec, respectively. Each event is shown on two different vertical scales so that the film profile can be seen clearly over the whole range of the film thickness variation. The theoretically predicted dynamic draining curves corresponding to $h_s \geqslant 2.3$ are shown in each case. It is seen in figures 9a and 9b that the agreement between theory and experiment is very good. In figure 9c a thin film above the surge is shown where the draining curve drops more sharply at first, which accords with the prediction for cases where $h_s \lesssim 2.0$.

It should be stated that although most of the film profiles caused by surges are similar to the theoretical prediction, there are often irregularities caused for example by the impingement of droplets near to the probe. At higher gas velocities ($V_G \sim 10$ m/sec) the film becomes wavy due to the shear forces of the gas phase. Under these circumstances, however, it is found that the film follows the predicted curve, but with the wave structure superimposed. For increased gas flow ($V_G \sim 20$ m/sec) it is found that the wavy film does not drain below a certain minimum thickness after a surge passes. Reduction of the liquid flow to a value $V_L \lesssim 0.25$ m/sec removes the surges, but a film is still maintained on the upper surface. This is not the case, however, at lower gas velocities. It is therefore concluded that when $V_G \gtrsim 20$ m/sec, the mechanisms of horizontal annular flow are strong enough to maintain the film whether surges are present or not.

7. CONCLUSIONS

The theory given here relies on a number of simplifying assumptions which are necessary because of the complex, highly disturbed structure of two-phase flow. For example, it is seen from figure 9 that the film thickness does not remain constant during the passage of a surge. Also the replenishment varies in intensity and is in the form of finite sized drops. Furthermore, the replenishment does not cease abruptly as assumed in the model. Other problems arise because of the waves caused by the gas flow and because no two surges are the same. Indeed individual surges are continually developing and changing their form as they progress along the tube. In spite of these and other difficulties it is found that the theory given here gives good agreement with experimental draining curves. In particular, the theory explains the observed initial rapid fall in film thickness which was not predicted by the "static" draining theory of Gardner (1972). The theory given here also predicts the initial thickness at the start of the draining process, provided it can be assumed that the thickness above the surge is greater than twice the characteristic thickness H_m. Since this is true for the vast majority of surges observed in the air–water experiments where $H_m = 0.285$ mm, it can also be expected to be true in high pressure steam–water flows where $H_m = 0.1$ mm.

Acknowledgement—This work was carried out at the Central Electricity Research Laboratories and is published by permission of the Central Electricity Generating Board.

REFERENCES

ALVES, G. E. 1954 Co-current liquid–gas flow in a pipe-line contactor. *Chem. Engng Prog.* **50**, 499–456.

BAKER, O. 1954 Simultaneous flow of oil and gas. *Oil & Gas J.* **53**, 185–195.

CONEY, M. W. E. 1973 The theory and application of conductance probes for the measurement of liquid film thickness in two-phase flow. *J. Phys. E. Sci. Instrum.* **6**, 9, 903–910.

GARDNER, G. C. 1972 Drainage and evaporation of a liquid film with salt deposition upon a horizontal cylindrical surface. *Int. J. Heat Mass Transfer* **15**, 2063–2075.

LIS, J. & STRICKLAND, J. A. 1970 Local variations of heat transfer in a horizontal steam evaporator tube. Paper B4.6, pp. 1–12. 4th International Heat Transfer Conference, Paris.

LUNN, D. C. F. & HARVEY, J. 1970 Corrosion at Trawsfynydd. *Engng* **209**, 189–191.

SAKIADIS, B. C. 1961 Boundary-layer behaviour on continuous solid surfaces, *A.I.Ch.E.J.* **7**, 221–225.

SCHICHT, H. H. 1969 Stromungsbilder bei adiabater Zweiphasenstromung Wasser/Luft in einem horizontalen Rohr. *Verfahrenstechnik* **3**, 153–161.

SCHLICHTING, H. 1968 *Boundary-Layer Theory*, 6th Edition. McGraw-Hill.

WEDEKIND, G. L. 1971 An experimental investigation into the oscillatory motion of the mixture–vapour transition point in horizontal evaporating flow. *Trans. ASME J. Heat Transfer* **93**, 47–57.

ZAHN, W. R. 1964 A visual study of two-phase flow while evaporating in horizontal tubes. *Trans. ASME J. Heat Transfer* **86**, 3, 417–429.

APPENDIX 1

The possibility of transition to a turbulent boundary layer (including consideration of the effect of a pressure gradient)

In this Appendix the assumption that the boundary layer is always laminar is examined. Consider the similar case of the boundary layer on a smooth flat plate. Experimental observations have indicated that transition to a turbulent boundary layer occurs when (Schlichting 1968, p. 454)

$$\frac{U_\infty D_1}{\nu} \simeq 950 \qquad [1.1]$$

where U_∞ is the free stream velocity above the flat plate and D_1 is the displacement thickness of the boundary layer. In terms of the dimensionless units used in this analysis, this suggests that transition would occur when

$$(u_o - u_b)\delta_1 \simeq 950. \qquad [1.2]$$

Since u_b is zero and δ_1 cannot be greater than about 0.69 (see figure 4), transition cannot take place unless $u_o > 1380$. This value corresponds to surge velocities of about 4.3 m/sec in an atmospheric air–water system or to between 1.6 and 2.0 m/sec in both high and low pressure boilers. All these values are quite likely to occur in practice.

It has been stated that there is an analogy between the effect of draining and the effect of suction on the development of the boundary layer, since both processes lead to a constant thickness and velocity profile. However, it has been pointed out to the author that this analogy does not extend to the question of stability, since the effects on the velocity profile are quite different. Suction causes an increase in the curvature of the velocity profile at the wall such that the critical condition for the onset of turbulence becomes (Schlichting 1968, p. 484)

$$\frac{U_\infty D_{1s}}{\nu} = 70000, \qquad [1.3]$$

where D_{1s} is the displacement thickness of the asymptotic suction profile. On the other hand draining has no effect on the curvature at the wall.

However, another important factor in the question of stability is the pressure gradient which has been neglected elsewhere in the analysis. If the pressure gradient is included, it may be shown that a modified velocity profile is obtained

$$\frac{u_o - u}{u_o - u_b} = \frac{2y}{b} - \frac{2y^3}{b^3} + \frac{y^4}{b^4} + \frac{\Omega}{6}\left(\frac{y}{b} - \frac{3y^2}{b^2} + \frac{3y^3}{b^3} - \frac{y^4}{b^4}\right) \qquad [1.4]$$

where Ω in this case is given by

$$\Omega = \frac{B^2}{\rho\nu(U_o - U_b)}\frac{\mathrm{d}P}{\mathrm{d}X}, \qquad [1.5]$$

where

$$U_b = u_b\frac{\nu}{H_m}$$

It is interesting to note from this result that in contrast to the problem of a boundary layer on a stationary wall, an adverse pressure gradient leads the velocity profile nearer to a parabolic shape and therefore into a region of greater stability.

Next, we make the assumption that the pressure gradient in the gas flowing over the surge is just sufficient to drive it along at its observed velocity U_o. Clearly the pressure gradient has to overcome the friction between the water in the surge and the lower part of the tube circumference, with which it is in contact. In addition, slow moving liquid must be continuously accelerated to the surge velocity in order to make up for the liquid thrown to the upper part of the tube and left behind when the surge has passed. Consideration of these two effects suggests that a reasonable approximation is obtained by calculating the pressure gradient in an annulus of liquid which is in contact with the whole perimeter of tube and is travelling at a velocity U_o. This yields the result that

$$\frac{\mathrm{d}P}{\mathrm{d}X} = \frac{\lambda_f \rho U_o^2}{2D}, \qquad [1.6]$$

where λ_f is the dimensionless coefficient of resistance and D is the tube diameter (m).

Combining [1.5] and [1.6], putting $U_b = 0$ and using the fact that $B = 2.3175\,H_m$, we obtain

$$\Omega = \frac{B^2\lambda U_o}{2\nu D} = 2.68\,\lambda_f U_o\sqrt{\frac{\rho}{\Delta\rho Rg}}. \qquad [1.7]$$

Taking $\rho = \Delta\rho = 1.0 \times 10^3\,\text{kg/m}^3$, $R = 0.025\,m$ and $\lambda_f = 0.025$, we find that when $U_o = 8$ m/sec, which is about the highest surge velocity observed in the C.E.R.L. air–water facility, $\Omega \simeq 1.0$.

Calculations described by Schlichting (1968, p. 471) predict that the theoretical critical Reynolds Number is raised from 645 to about 1200 when $\Omega = 1$. If in practice the Reynolds Number for transition is raised by the same factor, a value of 1770 is obtained. This is very close to the actual Reynolds Number obtained when $U_o = 8$ m/sec, suggesting that the boundary layer is at the point of transition at this velocity.

The estimation of the pressure gradient given here could be too low, because of effects such as the reduction of the flow area available to the gas and the entrainment of liquid into the gas flow. Nevertheless, especially in view of the turbulence in the outer flow, it must be concluded that transition to a turbulent boundary layer is a distinct possibility at high surge velocities (~ 8 m/sec). A further conclusion is that neglecting the effect of the pressure gradient on the boundary layer in the main analysis, appears to be a justifiable approximation except at high surge velocities, where Ω might become significantly greater than unity.

APPENDIX 2

The static draining theory

In this Appendix the equations of the static theory of viscous draining and evaporation are derived. The static equations may be derived from [62] directly, by putting ω and $d\omega/db = 0$. The results are as follows:

For $b \geqslant 1$,
$$t = 2 \ln \left[\frac{b_o - \frac{1}{3} + \frac{q}{2}}{b - \frac{1}{3} + \frac{q}{2}} \right] \qquad [2.1]$$

where $t = 0$ at the initial thickness b_o.

When $b < 1$, two cases must be considered, firstly that of $q = 0$, when
$$t = t_1 + \frac{3}{8}\left(\frac{1}{b^2} - 1\right) \qquad [2.2]$$

where t_1 is the time t when $b = 1$, and may be calculated from [2.1]. If $q > 0$, then for $b < 1$,
$$t = t_1 + F(1, b) \qquad [2.3]$$

where $F(\beta, b)$ is given by
$$F(\beta, b) = \frac{\alpha}{3q}\left[\frac{1}{2}\ln\frac{(\beta + \alpha)^2}{(b + \alpha)^2}\frac{(b^2 - \alpha b + \alpha^2)}{(\beta^2 - \alpha\beta + \alpha^2)} + \sqrt{3}\,\text{arctg}\frac{(2\beta - \alpha)}{\alpha\sqrt{3}} - \sqrt{3}\,\text{arctg}\frac{(2b - \alpha)}{\alpha\sqrt{3}}\right] \qquad [2.4]$$

and where
$$\alpha = \left(\frac{3}{4}q\right)^{1/3}$$

and β is an arbitrary constant.

If the initial thickness $b_o \leqslant 1$ and $q = 0$, then

$$t = \frac{3}{8}\left(\frac{1}{b^2} - \frac{1}{b_o^2}\right) \qquad [2.5]$$

and if $b_o \leqslant 1$, $q > 0$ then

$$t = F(b_o, b). \qquad [2.6]$$

Résumé—Il existe un régime d'écoulement diphasique dans lequel de grandes ondes ou des vagues déferlantes se propagent rapidement le long d'une conduite horizontale. Leur passage est accompagné d'éclaboussures, de rupture de vagues et d'entrainement, ce qui a pout résultat de projeter de l'eau sur la paroi supérieure de la conduite. Entre deux vagues, le film présent sur cette paroi supérieure s'appauvrit par écoulement dû à la gravité et par évaporation si la conduite est chauffée. Si l'intervalle entre les vagues est suffisamment long, une tache sèche peut commencer à se former. Dans cet article, on décrit une théorie qui calcule l'épaisseur du film après passage de vagues, et le temps nécessaire à l'assèchement. Le théorie inclut l'effet du développement de la couche limite durant l'alimentation du film, ainsi que l'effet de la décélération axiale de celui-ci au point où sou alimentation en liquide cesse. Finalement, la variation d'épaisseur de film calculée est comparée avec des enregistrements experimentaux obtenus avec ce type d'écoulement diphasique. L'accord s'avère très satisfaisant. L'intérêt de cette analyse est lié à la prévention des assèchements permanents ou intermittents aux faibles qualités dans les évaporateurs de centrales nucléaires de puissance.

Auszug—Es besteht eine Form der Zweiphasenstroemung, in der grosse Wellen oder Stoesse schnell laengs eines wagerechten Rohres entlang wandern. Dies wird von Spritzen, Wellenbrechen und Mitreissen begleitet, wodurch Wasser auf die Rohrscheiteloberflaeche geworfen wird. Zwischen den Stoessen verringert sich die Schicht auf der Scheiteloberflaeche durch Abfluss unter Schwerkraft, und durch Verdampfung, falls das Rohr beheizt wird. Wenn das Interval zwischen den Stoessen lang genug ist, kann sich ein trockener Fleck bilden. In diesem Aufsatz wird eine Theorie fuer die Berechnung der Restschichtdicke auf der Scheiteloberflaeche, und fuer die Berechnung der Zeit bis zum Trockenwerden, angegeben. Diese Theorie schliesst sowohl Effekte der Grenzschichtentwicklung waehrend der Wiederauffuellung der Schicht, wie auch die Wirkung der axialen Verzoegerung der Schicht ein, in dem Punkt in dem die Fluessigkeitswiederauffuellung endet. Schliesslich wird die vorhergesagte Veraenderung der Schichtdicke mit experimentellen Spuren der Schichtdicke verglichen, wie sie bei dieser Form von horizontaler Zweiphasenstroemung erhalten werden. Es wird sehr befriedigende Uebereinstimmung gefunden. Die Analyse ist von Interesse in Verbindung mit der Verhuetung von dauerndem oder unterbrockenem Trockenwerden bei niedrigen Dampfgehalten in Verdampfern von Kernkraftwerken.

Резюме—Показан режим двуфазного течения, в котором большие волны или валы быстро продвигаются вдоль горизонтальной трубы, что сопровождается расплескиванием, дроблением и затоплением волн, в результате чего вода забрасывается на верхнюю поверхность трубы. В промежутке медду валами верхняя поверхность очищается от пленки воды посредством дренирования под действием силы тяжести, а также испарением в случае нагретой трубы. В случае, если промежуток между валами достаточно долог, возможно начало формирования сухих участков. В данной статье дана теория для расчета толщины пленок, остающихся на верхних поверхностях, и времени их высыхания. Эта теория включает как влияние степени развития толщины граничного слоя во время наполнения пленки, так и влияние осевого уменьшения пленки в точке, где пополнение жидкостью прекращается. В заключение вычисленное изменение толщины пленки сравнивается с экспериментальными следами толщин пленки, полученными в этом типе горизонтального двуфазного потока. Совпадение данных найдено весьма удовлетворительным. Указанный анализ представляет интерес в целях предотвращения непрерывного или пульсирующего высыхания при низком качестве в испарителях ядерных электростанций.